Pergamon PII: S0038–092X(02)00019–1

Solar Energy Vol. 72, No. 5, pp. 385–395, 2002
© 2002 Published by Elsevier Science Ltd
Printed in Great Britain
0038-092X/02/$ - see front matter

www.elsevier.com/locate/solener

DYNAMIC ANNUAL DAYLIGHT SIMULATIONS BASED ON ONE-HOUR AND ONE-MINUTE MEANS OF IRRADIANCE DATA

OLIVER WALKENHORST[†,*], JOACHIM LUTHER[*], CHRISTOPH REINHART[**] and JENS TIMMER[***,****]

*Fraunhofer Institute for Solar Energy Systems ISE, Heidenhofstraße 2, 79110 Freiburg, Germany
**Institute for Research in Construction, National Research Council, 1200 Montreal Road, Ottawa, ON K1A 0R6, Canada
***Faculty of Physics, University of Freiburg, Hermann-Herder-Straße 3, 79104 Freiburg, Germany
****Center for Data Analysis and Modelling, University of Freiburg, Eckertstraße 1, 79104 Freiburg, Germany

Received 11 July 2001; revised version accepted 15 February 2002

Communicated by JEAN-LOUIS SCARTEZZINI

Abstract—This study investigates the influence of the short-term dynamics of daylight on simulation-based predictions of the annual daylight availability in a building. To this end annual indoor illuminance simulations are carried out for a two-person-office using the RADIANCE-based dynamic daylight simulation method DAYSIM. As of yet, all available daylight simulation methods are typically based on 1-h means of irradiance data and thus tend to neglect the short-term dynamics of daylight. In the first part of this study the dependence of the annual daylight availability on the underlying simulation time step interval is quantified. Assuming two different automated daylight-dependent artificial lighting strategies, the predicted annual artificial lighting demand is systematically underestimated by up to 27% on the simulations based on 1-h means instead of 1-min means of measured beam and diffuse irradiances. The general validity of these results is ensured by employing irradiance data from five stations world-wide. As measured 1-min means of irradiance data are generally not available for practical applications, the stochastic Skartveit–Olseth model, which generates 1-min means of irradiance data from hourly means, is adapted for daylight simulation purposes in the second part of this study. The utilization of modeled 1-min means of irradiance data reduces the above described systematic simulation errors to below 8% for both automated lighting strategies and all five stations. Accordingly, the modified version of the Skartveit–Olseth model is able to enhance the quality of dynamic daylight simulations — without any additional planning effort for the lighting designer. © 2002 Published by Elsevier Science Ltd.

1. INTRODUCTION

Within the present discussion dealing with new ideas on the construction of buildings the concept of a so-called *lean building* plays an increasing role (Voss *et al*., 2000). Lean buildings harmonize with their given climatic boundary conditions and exploit naturally available energy sinks and sources in order to provide increased thermal and visual comfort for their inhabitants while reducing the energy demand.

One aspect of a lean building is the conscious use of daylight to light the interior of buildings. The benefits of a carefully planned daylighting concept encompass an enhanced visual comfort for the inhabitants providing them with glare-free natural daylight and visual contact to the outside as well as a reduced electric energy demand for artificial lighting.

To compare different daylighting concepts during the planning phase of a building one has to rely on simulation methods that allow one to predict the annual daylight availability in the interior of a building. To this end the RADIANCE-based simulation environment DAYSIM which represents a reliable and easy-to-use tool to perform *dynamic indoor illuminance simulations* has recently been developed and validated (Reinhart and Herkel, 2000; Reinhart and Walkenhorst, 2001). Similar to the ESP-r/RADIANCE link (Janak, 1997) and the 'Dynamic Lighting System' (Cropper *et al*., 1997; Mardaljevic, 2000), DAYSIM is based on a daylight coefficient approach (Tregenza and Waters, 1983) and the Perez sky model (Perez *et al*., 1990, 1993). Daylight coefficient methods are able to simulate the time development of indoor illuminances for arbitrary time step intervals based on time series of beam and diffuse irradiances. As widely available test reference years usually provide hourly means, most dynamic daylight simu-

[†]Author to whom correspondence should be addressed; e-mail: walkenho@web.de

lation methods are presently based on this time step, i.e. the short-term dynamics of daylight introduced by clouds intermittently hiding the sun (see Fig. 1) or a temporarily varying cloud cover thickness is discarded. As daylight cannot be stored, the usage of 1-h irradiance data in dynamic daylight simulations may thus lead to considerable errors in the prediction of the annual daylight availability.

Janak suggested to use a stochastic model introduced by Skartveit and Olseth (Skartveit and Olseth, 1992) to model the intra-hour dynamics of the beam radiation and thereby reduce these errors (Janak, 1997). He implemented the Skartveit–Olseth model into ESP-r without further validating its applicability for dynamic daylight simulations. This paper extends Janaks original work by both quantifying the simulation errors introduced by using 1-h instead of 1-min time steps for annual daylight simulations (1) and by presenting and validating a practical method to reduce these simulation errors based on the Skartveit–Olseth approach (2):

1. Quantification of simulation errors with respect to time resolution: To quantify the errors in the prediction of the annual daylight availability which one incurs by neglecting the short-term dynamics of the daylight, dynamic annual indoor illuminance simulations are carried out for a test office with two different types of underlying irradiance data sets: *measured 1-h means* and *measured 1-min means*. The resulting two different types of annual indoor illuminance data sets are then used to predict the annual artificial lighting demand for two automated daylight-dependent lighting control strategies. Measured 1-min irradiance data sets are chosen as a lower threshold with respect to time resolution based on the assumption that they contain all information about the short-term dynamics of daylight which is relevant in the context of daylight simulations and as measured irradiance data with a higher time resolution are scarcely available.
2. Reduction of the simulation errors with respect to time resolution: Measured 1-min irradiance data are generally not available for practical applications. To reduce the simulation errors, 1-min irradiance data are modeled from hourly means using a modified version of the Skartveit–Olseth model (Skartveit and Olseth, 1992). This modified version is developed for use in dynamic daylight simulations. To quantify the error in the prediction of the annual daylight availability which remains if one uses modeled 1-min irradiance data, dynamic annual indoor illuminance simulations are carried out with *measured 1-min means* and *modeled 1-min means* of irradiance data as input. As in (1) the two resulting annual indoor illuminance data sets are then compared with respect to the predicted annual artificial lighting demand to ensure the capability of the modified Skartveit–Olseth model to reduce errors in dynamic daylight simulations. The organization of this paper is as follows: Section 2 describes the methodologies to investigate problems (1) and (2), simulation results are presented in Section

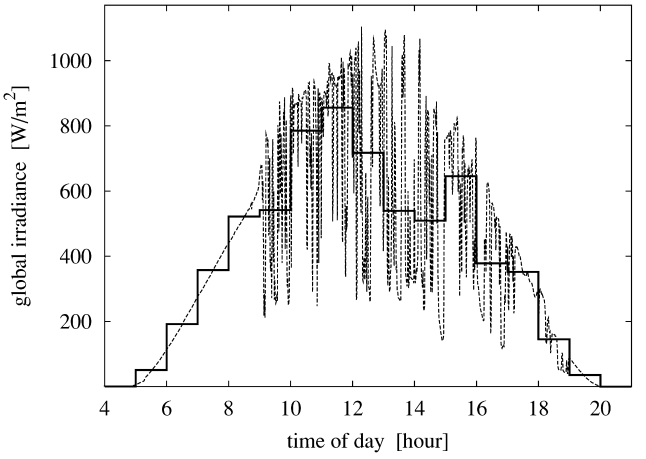

Fig. 1. Measured 1-h (solid line) and measured 1-min (dashed) means of global irradiance on May 17th 1998 in Freiburg, Germany.

3 and finally Section 4 contains concluding remarks and an outlook on remaining research tasks.

2. METHODOLOGY

2.1. Dynamic daylight simulations with DAYSIM

In this study all dynamic simulations of indoor illuminances due to daylight are performed using the RADIANCE-based simulation environment DAYSIM. DAYSIM merges the backward raytracer RADIANCE (Ward and Shakespeare, 1998) with a daylight coefficient approach and permits reliable and fast dynamic indoor illuminance simulations.

DAYSIM requires two essential informations for an annual indoor illuminance simulation:

(a) Description of the geometry and the materials of the building: This information is provided in the form of regular RADIANCE input files.

(b) Description of the light sources for each time step: Ambient daylight is physically described by the sky luminance distribution. As measurements of this two-dimensional function are usually not available for practical applications, DAYSIM makes use of the Perez sky luminous efficacy (Perez *et al*., 1990) and sky luminance distribution model (Perez *et al*., 1993) to model the sky luminance distribution using global and beam irradiance — which are widely available — as input values. Therefore DAYSIM needs to be fed with an annual data set of global and beam irradiances.

Given these two input files, DAYSIM allows one to simulate an annual indoor illuminance data set for any specified point and orientation inside of a given building. More details regarding the underlying simulation algorithm of DAYSIM are provided in Reinhart and Herkel (2000) and Reinhart (2001).

In the present study indoor illuminances are simulated for three simulation points inside and outside of a southward oriented 18 m^2 test office which is sketched in Fig. 2. Two simulation points inside the office are situated at work plane height on the middle axis of the office 2 and 4 m from the facade, both pointing upwards. They represent the work places of the two-person-office. The third simulation point is situated on the facade of the test office and points southward. All simulations are based on this test office. Only the underlying annual global and beam irradiance data sets are varied.

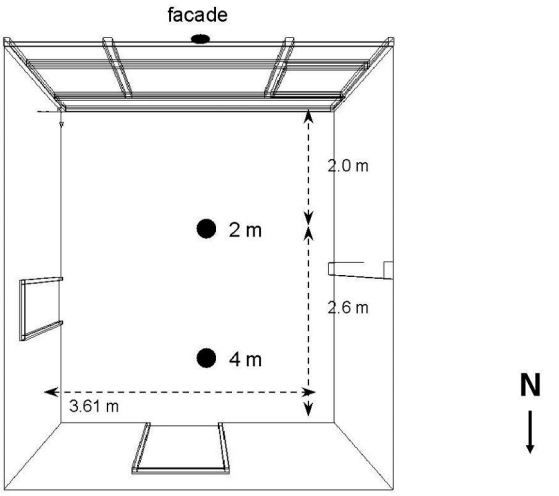

Fig. 2. Sketch of the test office including the position of the three simulation points.

2.2. Irradiance data sets

To examine the two problems described in the Introduction, annual indoor illuminance simulations are carried out for three different global and beam irradiance data sets:

- measured 1-min means (1)
- measured 1-h means (2)
- modeled 1-min means (3)

Fig. 3 provides a schematic survey of the daylight simulations and the underlying irradiance data sets employed in this study.

2.2.1. Measured 1-min means. Measured 1-min means of global and beam irradiances are the basic irradiance data set from which the other two sets, measured 1-h means and modeled 1-min means, are derived.

To support the general validity of the simulation results, eight annual data sets of measured 1-min global and beam irradiance from five different weather stations world-wide are used. The five stations are listed in Table 1.

All five stations are affiliated to the International Daylight Measurement Programme (IDMP)[†] launched by the CIE in 1991.

2.2.2. Measured 1-h means. Each of the eight annual data sets of measured 1-min global and beam irradiance described in the previous subsec-

[†]http://idmp.entpe.fr

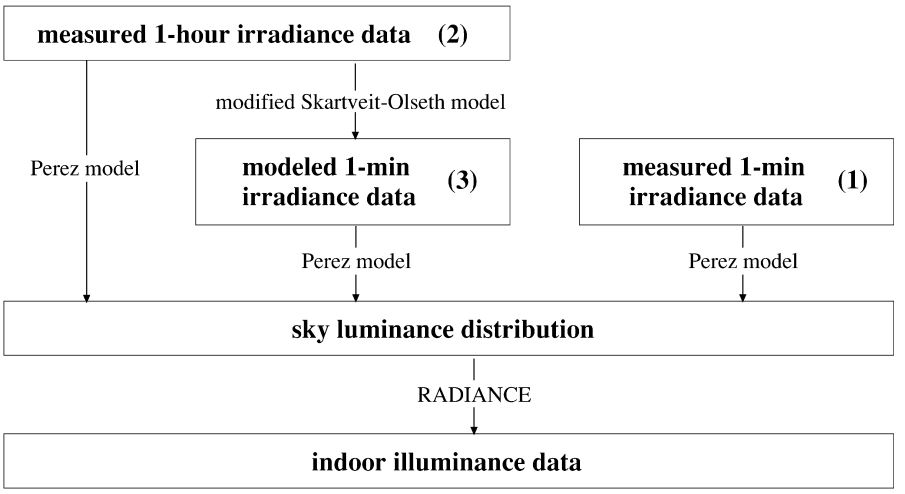

Fig. 3. Schematic survey of the simulation pathways in the present study. The numbers pertain to the enumeration in the text.

tion yields — by averaging — an annual data set of measured 1-h global and beam irradiance.

2.2.3. Modeled 1-min means. In this study a modified version of the stochastic Skartveit–Olseth model is used to generate 1-min global and beam irradiance data from measured hourly means. The basic structure of the original Skartveit–Olseth is sketched in the following. The model consists of seven steps which are carried out for each hour of the year with non-vanishing ambient irradiances:

1. Input: 1-h means of global irradiance $K \leq 0.3$ and beam irradiance $0.3 < K \leq 0.6$.
2. Transformation to relative quantities using the McMaster clear sky model (Davies and McKay, 1982) which results in 1-h means of the so-called global clearness index $K = G/G_c$ and beam clearness index $K_b = G_b/G_{bc}$.
3. Realization of the intra-hour standard deviation $\sigma_k = (\Sigma_{i=1}^{60} (k_i - K)^2)^{1/2}$ and $\sigma_{k_b} = (\Sigma_{i=1}^{60} (k_{b,i} - K_b)^2)^{1/2}$ of the 60 1-min global and beam clearness indices k_i and $k_{b,i}$ using a parametrized probability distribution.
4. Realization of 60 1-min global and beam clearness indices k_i and $k_{b,i}$ using parametrized probability distributions.
5. Temporal rearrangement of the 60 1-min global and beam clearness indices using realizations of a first order autoregressive process (AR(1) process, see, e.g. Brockwell and Davis, 1991).
6. Back-transformation to absolute quantities using the McMaster clear sky model which results in 1-min global irradiances $g_i = k_i \cdot g_{c,i}$ and beam irradiances $g_{b,i} = k_{b,i} \cdot g_{bc,i}$.
7. Output: 60 1-min means of global irradiance g_i and beam irradiance $g_{b,i}$ ($i = 1, \ldots, 60$).

The output 1-min global and beam irradiances for each hour are then concatenated hour by hour. This way one can obtain annual data sets of modeled 1-min global and beam irradiance from data sets of hourly means. The reader should bear in mind that the Skartveit–Olseth model is stochastic, i.e. different initializations of the employed pseudo-random number generator result in different realizations of annual 1-min irradiance data sets.

While preserving the basic structure of the original Skartveit–Olseth model, the following five modifications have been carried out to render the model more suitable for dynamic indoor illuminance simulations:

1. Synchronization of global and beam irradiances: As mentioned above DAYSIM employs the Perez sky luminance distribution model which requires consistent global and beam irradiance as input, i.e. global and beam irradiances have to be mutually matched at each time step. In the original Skartveit–Olseth

Table 1. Latitudes, longitudes and station heights of the five weather stations (a.s.l. = above sea level)

Station	Latitude [°]	Longitude [°]	Height [m a.s.l.]
Albany/USA	42.70 N	73.85 W	79
Bratislava/Slovakia	48.17 N	17.08 E	195
Freiburg/Germany	47.98 N	7.83 E	279
Geneve/Switzerland	46.33 N	6.02 E	425
Tsukuba/Japan	36.15 N	140.05 E	43

model the output 1-min global and beam irradiances are put in order according to two independent AR(1) processes and are thus not synchronized. Therefore it may happen that for a single time step the beam irradiance exceeds the global irradiance which leads to a negative diffuse irradiance. To obtain consistent 1-min global and beam irradiances, the Reindl model (Reindl *et al*., 1990) which estimates the diffuse fraction of a given global irradiance is used instead in this study. The Reindl model is used in its simplest version which merely requires global irradiance and solar elevation as input parameters. In the modified Skartveit–Olseth model steps (2)–(6) are solely performed for the global irradiance and between step (6) and step (7) the Reindl model is utilized to determine the beam irradiance at each time step.

2. Usage of the ESRA clear sky model: To reduce the number of required site-specific atmospheric input parameters for the clear sky model — which are not available for arbitrary sites — the ESRA clear sky model (Rigollier *et al*., 2000) is employed in step (2) and step (6) to replace the McMaster clear sky model. The ESRA model is a broadband model which predicts global and beam irradiance for a given site and time under clear sky conditions. It requires the Linke turbidity factor, which summarizes the overall turbidity of the atmosphere, as the only atmospheric input parameter. In addition, the monthly mean Linke turbidity factors for a given site can be estimated from the input hourly means of beam irradiance[†]. Thus the input of site-specific atmospheric parameters becomes optional which makes the modified Skartveit–Olseth model easier to use for practical applications. An investigation based on the eight annual data sets of 1-min global irradiance showed that ESRA model and McMaster model yield very similar global clearness indices. As, due to modification (1), the modified Skartveit–Olseth model is solely based on global clearness indices, the replacement of the McMaster model with the ESRA model scarcely influences the suitability of the original probability distributions.
3. New parametrizations to improve the modeling of the minima of the 1-min global indices: A thorough analysis based on the eight annual data sets of measured and modeled 1-min global irradiances indicated that the original Skartveit–Olseth model generates too many very small 1-min global indices, especially outliers below $k_i = 0.2$. Dynamic indoor illuminance simulations aiming at the prediction of the annual daylight availability are very sensitive to this type of shortcoming as too many extreme global irradiance minima result in an underestimation of the annual daylight availability and consequently in an overestimation of the annual artificial lighting demand. Therefore, a new parametrization of the three relations $\sigma_k^*(K, \sigma_3)$, $k_{\min}(K, \sigma_k)$ and $k_{\max}(K, \sigma_k)$ (Eqs. (6b), (9b) and (9c) in Skartveit and Olseth, 1992) which pertain to step (3) and step (4) of the original model) was necessary as these three quantities determine the extrema of the 1-min global clearness indices of each hour, using the average root squared deviation of the 3-h global clearness indices of the preceeding, the actual and the following hour, σ_3. For the new parametrization the following approach has been chosen for the three relations:

$$\sigma_k^{*(\mathrm{new})}(K, \sigma_3) = \beta_\sigma \cdot \sigma_k^*(K, \sigma_3) \tag{1}$$

$$k_{\min}^{(\mathrm{new})} = (K - 0.03) \cdot \exp(-11 \cdot \beta_{\min} \cdot \sigma_k^{1.4}) - 0.09 \tag{2}$$

$$k_{\max}^{(\mathrm{new})} = (K - 1.5) \cdot \exp(-9 \cdot \beta_{\max} \cdot \sigma_k^{1.3}) + 1.5 \tag{3}$$

This approach originates from a careful comparison of the eight annual data sets of measured and modeled (using the original Skartveit–Olseth model) 1-min global irradiances. The three parameters β_σ, $\beta_{\min}$ and $\beta_{\max}$ have been determined on the basis of the eight annual data sets by minimizing a suitable objective function. For the objective function the sum of the squared relative deviations between the smallest measured and the smallest modeled 1-min global clearness index of each hour plus the same sum of the deviations between the biggest 1-min global clearness indices of each hour was used. To allow for a more flexible adjustment of the three parameters the minimization has been carried out separately for four different clearness index classes to which

[†]To estimate the monthly mean Linke turbidity factors we have used an empirically based algorithm which calculates the Linke turbidity factor for the 4 h of each day with the highest solar elevation by inverting the ESRA formula for the clear sky beam irradiance. From about the 120 calculated hourly Linke turbidity factors for each month the smallest three are then selected and the mean of these serves as an approximation for the monthly mean Linke turbidity factor for this month.

every hour has previously been assigned to according to its hourly mean of the global clearness index. Table 2 contains the results for the three parameters for all four clearness index classes.

4. Minimization of artificial discontinuities between subsequent hours: In the original Skartveit–Olseth model the realizations of the AR(1) process for the temporal rearrangement of the 1-min global clearness indices (step (5)) are completely independent for subsequent hours. Therefore, artificial discontinuities usually arise at the transition between subsequent hours. To minimize these artificial discontinuities, special realizations of the AR(1) process are selected. The AR(1) realization selected for each hour depends on the last 1-min global clearness index of the preceeding hour: one chooses the AR(1) realization in which that 1-min global clearness index of the current hour with the smallest difference to the last 1-min global clearness index of the preceeding hour is arranged at the first position of the current hour.
5. Input option for a horizon: The modified Skartveit–Olseth model allows to input the horizon of the simulation site which may consist of mountains or surrounding buildings. If this information is available the horizon can be entered via 36 horizon heights which represent azimuth segments of 10° width. Considering the horizon can reduce artifacts in the hours when the sun is partly below the horizon by taking into account the absence of beam irradiance during time steps when the sun is hidden behind the horizon. On the one hand it becomes possible to calculate hourly global clearness indices more accurately in step (2) and on the other hand the output 1-min irradiances in step (7) become more precise.

To run the modified Skartveit–Olseth model requires no additional information besides the geographic coordinates of the simulation site. The generation of an annual 1-min irradiance data set from hourly means requires about 90 s on a Pentium Pro 200 MHz Linux workstation.

The modified Skartveit–Olseth model can also be run at several coarser time steps ranging between 2 and 30 min by averaging the originally generated 1-min data but has not explicitly been validated with measured data in this range.

Table 2. Results for the three new fitting parameters for each of the four clearness index classes (K is the hourly mean global clearness index)

	$K \leq 0.3$	$0.3 < K \leq 0.6$	$0.6 < K \leq 0.9$	$K > 0.9$
β_σ	1.3	1.3	1.0	0.7
$\beta_{\min}$	−0.03	0.20	0.47	2.00
$\beta_{\max}$	1.66	4.26	0.89	0.38

2.3. Comparison of the resulting simulated illuminance data sets

The three different types of annual irradiance data sets described in Section 2.2 result in three different simulated annual illuminance data sets for the three simulation points inside and outside of the test office.

These three annual illuminance data sets are of different practical relevance:

1. The simulated illuminances based on measured 1-min irradiance data are of limited relevance for practical applications due to the lack of available measured 1-min irradiance data, but they serve as a reference case in the following comparison. An accompanying study showed that they are in good agreement with measured illuminances in the test office.
2. The simulated illuminances based on measured 1-h irradiance data represent the time resolution of conventional dynamic indoor illuminance simulations using test reference years.
3. The simulated illuminances based on modeled 1-min irradiance data using the modified Skartveit–Olseth model constitute a new possibility to cope with the short-term dynamics of daylight. They are derived from data set (2).

The criterion which is chosen to compare these three different illuminance data sets is the annual electric energy demand for artificial lighting using the following two different automated lighting control strategies:

(a) The *closed loop* strategy operates with two ceiling-mounted lamps with integrated illuminance sensors facing downward which are ideally calibrated and measure the simulated illuminance on the two work plane positions at 2 and 4 m distance from the facade. As soon as one simulated work plane illuminance falls below a given threshold illuminance the dimmed lamp lighting this work plane instantaneously provides the lacking illuminance to maintain the threshold illuminance.

(b) The *facade sensor* strategy operates with two ceiling-mounted lamps and one facade-mounted illuminance sensor facing southward which measures the simulated southward outdoor illuminance. To any given indoor threshold illuminance corresponds a much larger outdoor threshold illuminance which is different for the two work plane positions. As soon as the simu-

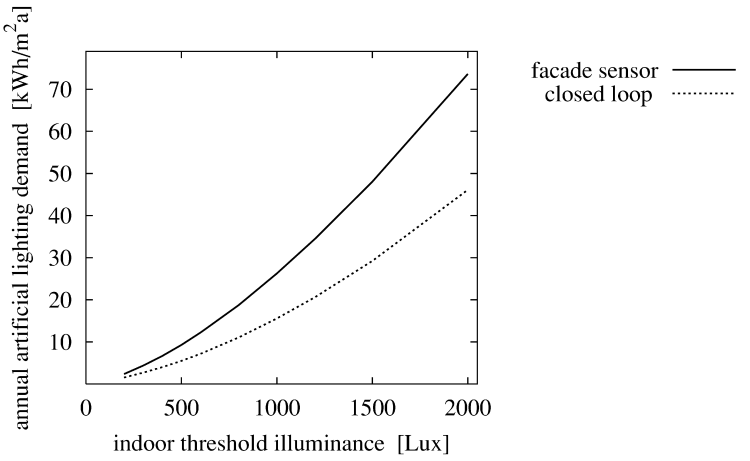

Fig. 4. Predicted specific annual electric energy demand for artificial lighting assuming the *facade sensor* and *closed loop* strategy on the basis of measured 1-min irradiance data vs. the indoor threshold illuminance for Freiburg (1998).

lated southward outdoor illuminance falls below the outdoor threshold illuminance of either of the two lamps, the corresponding lighting system is fully switched on. Moreover, the lamp remains activated for at least 15 min after being activated. This inertia of the system is introduced to supress frequent and irritating switchings of the lamps in the presence of temporarily varying clouds.

Both control strategies do not take into account any glare protection systems or shading devices.

More precisely, as criterion the specific[†] annual electric energy demand for artificial lighting of the whole test office is calculated for both strategies which is measured in kW h per net office area and year. The mean for the whole test office is obtained by averaging the specific energy demand of the two separately treated simulation points with their respective lamps. To enhance the general validity of the investigations, the annual electric energy demands are computed for a wide range of given indoor threshold illuminances I_t within 200 and 2000 Lux (e.g. in Germany for a small office a minimum of 500 Lux is prescribed by code (DIN, 1990)). Depending on the indoor threshold illuminance I_t, the specific delivery rate of the lamps P_s is set to

$$P_s(I_t) = 2.5\,\mathrm{W/m^2} + 0.025(\mathrm{W/m^2})/\mathrm{Lux} \cdot I_t \qquad (4)$$

following the reference of the Swiss Society of Engineers and Architects dealing with energy in building construction (SIA, 1995). The first term of Eq. (4) pertains to an electronic ballast. Finally, the attendance time of the work places is assumed to be weekdays between 8 a.m and 6 p.m. Fig. 4 illustrates the order of magnitude of the specific annual electric energy demand for the two strategies vs. the underlying threshold illuminance.

Some remarks concerning the criterions will conclude this section. The two automated lighting control strategies are chosen because they cover a wide range of possible automated daylight-dependent artificial lighting strategies: on one side *closed loop* as a dimmed and instantaneously reacting strategy and on the other side *facade sensor* as an undimmed and inertial strategy. The authors do not imply that the investigated systems represent the most common automated lighting systems which are in use nowadays.

In this study only *automated* strategies as opposed to *manual control* strategies are considered because validated models for manual control strategies are currently not available. The development of such models will be part of the newly proposed IEA task 31, which will focuss on the influence of the occupants on the daylight availability in a building. The authors assume that 1-h illuminance data will presumably be insufficient to model manual control strategies so that short-term illuminance data — whose generation is enabled by means of this study — will be required by these models.

It is worthwhile to mention that the annual electric energy demand for artificial lighting is only *one* possible measure for the annual daylight availability. But every other possible measure will supposedly depend in a similar way on the time resolution of the illuminance data. Their sensitivi-

[†]In this study 'specific' means 'based on the footprint'.

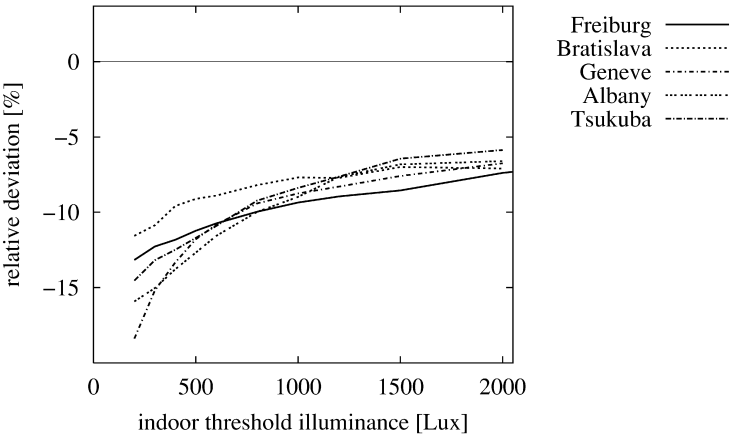

Fig. 5. Relative deviation according to Eq. (5) for the *closed loop* lighting control strategy vs. the indoor illuminance threshold for 1 year of data from each of the stations Freiburg (1998), Bratislava (1998), Geneve (1999), Albany (1996) and Tsukuba (1994).

ty to time resolution may be smaller or even larger than the sensitivity of the artificial lighting demand presented in the following section.

3. RESULTS

This section presents the results of the comparison of the three different simulated illuminance data sets. In Section 3.1 simulation errors of the annual artificial lighting demand due to reduced time resolutions are quantified. Section 3.2 shows how far these prediction errors can be reduced using the modified Skartveit–Olseth model.

3.1. Quantification of simulation errors with respect to time resolution

In the following simulated annual illuminance data sets based on *measured 1-h* and *measured 1-min* irradiance data are compared to each other with respect to predicted specific annual electric energy demand for artificial lighting for the above described office scenarios.

Fig. 5 presents results for the *closed loop* strategy for the five investigated sites and varying indoor illuminance thresholds. The figure shows the specific annual electric energy demand for artificial lighting based on measured 1-h irradiance data, $W_{\text{1-h,measured}}$, to measured 1-min irradiance data, $W_{\text{1-min,measured}}$. To facilitate the comparison between different stations, relative deviations

$$\Delta_{\text{rel}} = (W_{\text{1-h,measured}} - W_{\text{1-min,measured}})/W_{\text{1-min,measured}} \tag{5}$$

are plotted.

Fig. 6 displays the same results for the *facade sensor* strategy. The two figures reveal that for

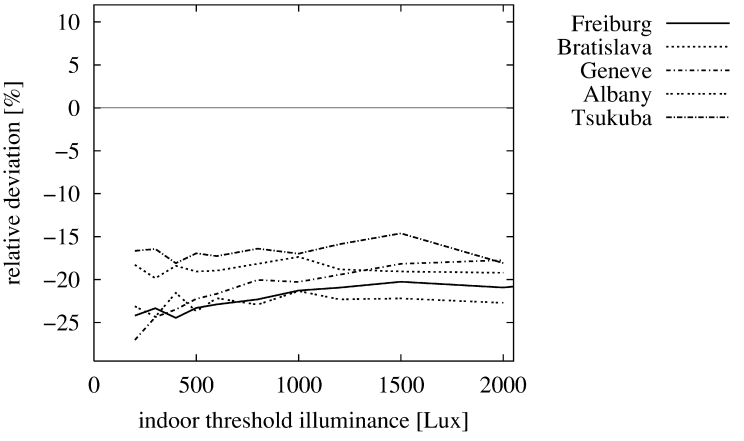

Fig. 6. Relative deviation according to Eq. (5) for the *facade sensor* lighting control strategy vs. the indoor illuminance threshold for 1 year of data from each of the stations Freiburg (1998), Bratislava (1998), Geneve (1999), Albany (1996) and Tsukuba (1994).

both lighting control strategies and all investigated sites the annual artificial lighting demand is systematically underestimated using 1-h instead of 1-min irradiance data. This systematic underestimation lies for all stations and for all investigated threshold illuminances within the range of 6–18% for the *closed loop* strategy and within the range of 15–27% for the *facade sensor* strategy.

This effect is primarily caused by the fact that during most annual working hours the hourly mean illuminance exceeds the considered threshold illuminances. For these hours the simulation based on 1-h means predicts sufficient daylight during the whole hour whereas 1-min illuminances may occasionally fall below the threshold illuminance thereby activating the artificial lighting system. During these hours one can only 'forfeit daylight' if one simulates with a time resolution of 1 min compared to hourly simulations. This forfeiture has a stronger influence on the *facade sensor* than on the *closed loop* strategy as for the former one single 1-min illuminance that lies below the threshold illuminance results in 15 min of activated artificial lighting due to the built in inertia of the control system.

We also analyzed the seasonal variability of the relative deviation for different indoor illuminance thresholds. We found that for low indoor illuminance thresholds ($<$500 Lux) the largest part of the overall annual relative deviation stems from the winter months. For increasing indoor illuminance thresholds the winter share of the overall annual relative error decreases until the summer share becomes the dominant part of the overall annual relative error for high indoor illuminance thresholds (2000 Lux). This is due to the fact that winter hours are on average darker than summer hours, i.e. intra-hour indoor illuminances tend to scatter around rather low values ($<$500 Lux) in winter and around rather high values (2000 Lux) in summer.

3.2. Reduction of simulation errors with respect to time resolution

In this section simulation results based on *modeled 1-min* and *measured 1-min* irradiance data are compared.

Figs. 7 and 8 correspond to Figs. 5 and 6 from the preceeding section. They reveal that for both lighting control strategies and all investigated sites the time-resolution-related simulation errors are significantly reduced using the modified Skartveit–Olseth model. The remaining errors amount to less than 2% for the *closed loop* strategy and to less than 8% for the *facade sensor* strategy for all considered sites and all investigated illuminance thresholds.

The remaining overestimation for the *facade sensor* strategy originates from the tendency of the modified Skartveit–Olseth model to still generate too many very small 1-min irradiances. Without the improved parametrization explained under 2.3.3 the overestimation for the *facade sensor* strategy would lie above 20%.

However, the remaining errors are small if one keeps in mind that the annual outdoor solar irradiance supply at one fixed site varies by around $\pm$10% (Reise, 2001) and thus leads to natural variations of the annual daylight availability for different years.

For the potential user of the model it is important to mention that different realizations of the modeled annual 1-min irradiance data, i.e. different runs of the stochastic Skartveit–Olseth model, only have a minor impact on the simulation outcome. The relative standard deviation of

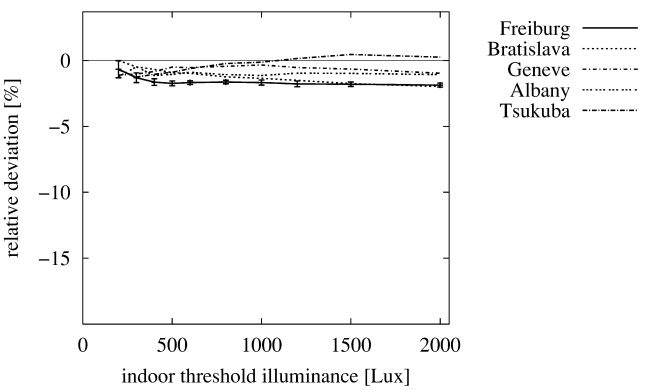

Fig. 7. Relative deviation between modeled and measured 1-min irradiance data in analogy to Eq. (5) for the *closed loop* lighting control strategy vs. the indoor illuminance threshold for 1 year of data from each of the stations Freiburg (1998), Bratislava (1998), Geneve (1999), Albany (1996) and Tsukuba (1994).

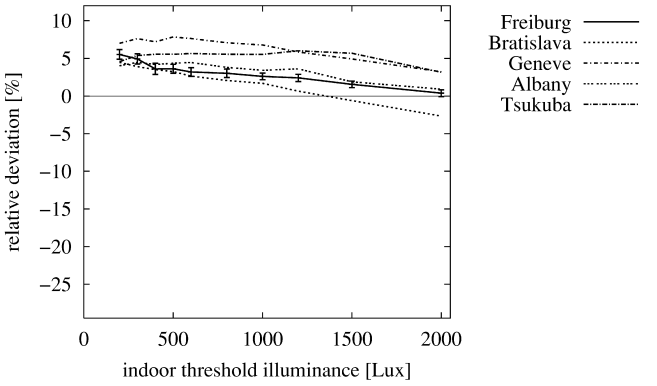

Fig. 8. Relative deviation between modeled and measured 1-min irradiance data in analogy to Eq. (5) for the *facade sensor* lighting control system vs. the indoor illuminance threshold for 1 year of data from each of the stations Freiburg (1998), Bratislava (1998), Geneve (1999), Albany (1996) and Tsukuba (1994).

the specific annual electric energy demand for artificial lighting resulting from ten different realizations never surmounts 0.7% for all stations, investigated threshold illuminances and lighting strategies. This implies that for practical purposes one single realization of the model should usually yield a sufficient simulation accuracy.

4. CONCLUSION

This study shows that the neglection of the short-term dynamics of natural daylight can introduce substantial errors in the simulation of the specific annual electric energy demand for automated control strategies of artificial lighting systems. These systematic errors can be significantly reduced if one simulates indoor illuminances based on modeled 1-min irradiance data using the modified Skartveit–Olseth model.

The authors' confidence in the general applicability of the modified Skartveit–Olseth model for dynamic daylight simulations is based on the following three arguments:

- The employed data stem from five stations worldwide which are situated in diverse climates within densely populated regions. For all these sites a comparable quality of simulation results has been achieved.
- Further simulations have confirmed that this high quality could be maintained for other office geometries with smaller facade apertures, room depth up to 10 m and varying facade orientations. There is a tendency towards increased simulation errors with increasing brightness of the office, i.e. the brighter the office the bigger the relative discrepancy between simulations based on 1-h and 1-min irradiance data. This is due to the fact that in brighter offices more hourly indoor illuminances lie above the threshold illuminance.
- The investigated indoor illuminance thresholds comprise the wide range between 200 and 2000 Lux which covers the complete range which is thought to be relevant for daylighting.

The modified Skartveit–Olseth model is easy to use as it requires only marginal user input and thus allows a more accurate prediction of daylight-relevant planning quantities without any additional working effort for the lighting designer compared to conventional dynamic daylight simulations based on hourly data. The modified Skartveit–Olseth model as well as the DAYSIM simulation environment can be downloaded from www.nrc.ca/irc/ie/light/daysim.html.

Finally we give an outlook on further possible applications of modeled 1-min irradiance data:

1. This study focusses on the differences between 1-h and 1-min irradiance data concentrating on the distribution of intra-hour minima. The distribution of intra-hour irradiance *maxima* presumably also depends on the time resolution of the data. For this reason modeled 1-min irradiance data could be used for enhanced predictions of the frequency of glare effects which might in turn lead to an enhanced performance assessment of shading devices.
2. As mentioned in Section 2.3 the modeling of *manual control strategies* for both artificial lighting systems and shading devices necessitates short-term irradiance data.
3. More generally, short-term irradiance data might be of use in modeling any kind of *non-linear solar-driven system,* especially if it exhibits a threshold behaviour as, e.g. solar thermal devices or photovoltaic pumping systems.

NOMENCLATURE

g_i	1-min global irradiance pertaining to the ith minute [W/m^2]
$g_{b,i}$	1-min beam irradiance pertaining to the ith minute [W/m^2]
$g_{bc,i}$	1-min beam irradiance under clear sky pertaining to the ith minute [W/m^2]
$g_{c,i}$	1-min global irradiance under clear sky pertaining to the ith minute [W/m^2]
G	1-h global irradiance [W/m^2]
G_b	1-h beam irradiance [W/m^2]
G_{bc}	1-h beam irradiance under clear sky [W/m^2]
G_c	1-h global irradiance under clear sky [W/m^2]
I_t	indoor threshold illuminance [Lux]
k_i	1-min global clearness index pertaining to the ith minute [–]
$k_{b,i}$	1-min beam clearness index pertaining to the ith minute [–]
k_{max}	upper threshold for 1-min global clearness indices during hour [–]
$k_{max}^{(new)}$	upper threshold for 1-min global clearness indices during hour (according to new parametrization) [–]
k_{min}	lower threshold for 1-min global clearness indices during hour [–]
$k_{min}^{(new)}$	lower threshold for 1-min global clearness indices during hour (according to new parametrization) [–]
K	1-h global clearness index [–]
K_b	1-h beam clearness index [–]
P_s	specific delivery rate of the lamps [W/m^2]
$W_{1\text{-h,measured}}$	specific annual electric energy demand for artificial lighting based on measured 1-h irradiance data [kW h/m^{2}a]
$W_{1\text{-min,measured}}$	specific annual electric energy demand for artificial lighting based on measured 1-min irradiance data [kW h/m^{2}a]
β_σ	fitting parameter [–]
β_{max}	fitting parameter [–]
β_{min}	fitting parameter [–]
Δ_{rel}	relative deviation with respect to the predicted specific annual electric energy demand for artificial lighting [–]
σ_3	average root squared deviation between the hourly global clearness indices of three subsequent hours [–]
σ_k	standard deviation of 1-min global clearness indices during 1 h [–]
σ_k^*	expectation value of the standard deviation of 1-min global clearness indices during 1 h [–]
$\sigma_k^{*(new)}$	expectation value of the standard deviation of 1-min global clearness indices during 1 h (according to new parametrization) [–]
σ_{k_b}	standard deviation of 1-min beam clearness indices during 1 h [–]

Acknowledgements—We would like to thank Arvid Skartveit and Jan Asle Olseth for making the source code of their original model available and to Guy Newsham for providing valuable comments on a draft version of this paper. Many thanks to Christian Reise, Stanislav Darula and Richard Kittler, Pierre Ineichen, Tsunebumi Mikuni and Richard Perez for sharing their irradiance data with us.

Finally the authors are indepted to their colleagues at the Solar Building Design Group at the Fraunhofer Institute for Solar Energy Systems for valuable comments and fruitful discussions.

REFERENCES

Brockwell P. J. and Davis R. A. (1991). *Time Series: Theory and Methods*, Springer, New York.

Cropper P., Lomas K. J., Lyons A. and Mardaljevic, J. (1997) A Dynamic Lighting System: Background and Prototype. *LuxEuropa 97 Proceedings*, Amsterdam, pp. 480–492.

Davies J. A. and McKay D. C. (1982) Estimating solar irradiance and components. *Solar Energy* **29**(1), 55–64.

DIN (1990) DIN 5035, Teil 2: Beleuchtung mit künstlichem Licht, Richtwerte für Arbeitsstätten in Innenräumen und im Freien.

Janak M. (1997). Coupling building energy and lighting simulation. *Fifth International IBPSA Conference*, Prague, 8–10 September 1997, Vol. II, pp. 313–319.

Mardaljevic J. (2000) Simulation of annual daylighting profiles for internal illuminances. *Light. Res. Technol.* **32**(3), 111–118.

Perez R., Ineichen P., Seals R., Michalsky J. and Stewart R. (1990) Modeling daylight availability and irradiance components from direct and global irradiance. *Solar Energy* **44**(5), 271–289.

Perez R., Seals R. and Michalsky J. (1993) All-weather model for sky luminance distribution — preliminary configuration and validation. *Solar Energy* **50**, 235–245.

Reindl D. T., Beckman W. A. and Duffie J. A. (1990) Diffuse fraction correlations. *Solar Energy* **45**(1), 1–7.

Reinhart C. F. and Herkel S. (2000) The simulation of annual daylight illuminance distributions — a state-of-the-art comparison of six RADIANCE-based methods. *Energy Build.* **32**, 167–187.

Reinhart C. F. and Walkenhorst O. (2001) Validation of dynamic RADIANCE-based daylight simulations for a test office with external blinds. *Energy Build.* **33**, 683–697.

Reinhart C. F. (2001) Daylight Availability and Manual Lighting Control in Office Buildings — Simulation Studies and Analysis of Measurements. Ph.D. Thesis, Technical University of Karlsruhe, Germany, ISBN 3-8167-6056-2.

Reise C. (2001) Private communication.

Rigollier C., Bauer O. and Wald L. (2000) On the clear sky model of the ESRA — European Solar Radiation Atlas — with respect to the heliosat method. *Solar Energy* **68**, 33–45.

SIA (1995) Empfehlung SIA 380/4: Elektrische Energie im Hochbau. Schweizerischer Ingenieur-und Architekten-Verein.

Skartveit A. and Olseth J. A. (1992) The probability density and autocorrelation of short-term global and beam irradiance. *Solar Energy* **49**(6), 477–487.

Tregenza P. R. and Waters I. M. (1983) Daylight coefficients. *Light. Res. Technol.* **15**(2), 65–71.

Voss K., Reinhart C. F., Löhnert G., Wagner A. (2000) Towards lean buildings — examples and experience from a German demonstration program for energy efficiency and solar energy use in commercial buildings. *Conference Proceedings of the EUROSUN*, Kopenhagen, 19–22 June 2000, CD-ROM.

Ward G. and Shakespeare R. (1998). *Rendering with RADIANCE. The Art and Science of Lighting Visualization*, Morgan Kaufmann Publishers.